Assessment and adjustment of sea surface salinity products from Aquarius in the southeast Indian Ocean based on *in situ* measurement and MyOcean modeled data

XIA Shenzhen[1, 2, 3], KE Changqing[1, 2, 3*], ZHOU Xiaobing[4], ZHANG Jie[5]

[1] Jiangsu Provincial Key Laboratory of Geographic Information Science and Technology, Nanjing University, Nanjing 210023, China

[2] Collaborative Innovation Center of South China Sea Studies, Nanjing 210023, China

[3] Collaborative Innovation Center of Novel Software Technology and Industrialization, Nanjing 210023, China

[4] Department of Geophysical Engineering, Montana Tech of the University of Montana, Butte, MT 59701, USA

[5] The First Institute of Oceanography, State Oceanic Administration, Qingdao 266061, China

Abstract

The *in situ* sea surface salinity (SSS) measurements from a scientific cruise to the western zone of the southeast Indian Ocean covering 30°–60°S, 80°–120°E are used to assess the SSS retrieved from Aquarius (Aquarius SSS). Wind speed and sea surface temperature (SST) affect the SSS estimates based on passive microwave radiation within the mid- to low-latitude southeast Indian Ocean. The relationships among the *in situ*, Aquarius SSS and wind-SST corrections are used to adjust the Aquarius SSS. The adjusted Aquarius SSS are compared with the SSS data from MyOcean model. Results show that: (1) Before adjustment: compared with MyOcean SSS, the Aquarius SSS in most of the sea areas is higher; but lower in the low-temperature sea areas located at the south of 55°S and west of 98°E. The Aquarius SSS is generally higher by 0.42 on average for the southeast Indian Ocean. (2) After adjustment: the adjustment greatly counteracts the impact of high wind speeds and improves the overall accuracy of the retrieved salinity (the mean absolute error of the Zonal mean is improved by 0.06, and the mean error is -0.05 compared with MyOcean SSS). Near the latitude 42°S, the adjusted SSS is well consistent with the MyOcean and the difference is approximately 0.004.

Key words: Aquarius, sea surface salinity (SSS), *in situ* SSS, MyOcean, comparison analysis, southeast Indian Ocean

---

1 Introduction

Oceans are a dominant component of the global water cycle; land runoff flows into the oceans, 78% and 86% of the world's precipitation and evaporation, respectively, occur over the oceans (Schmitt, 2008). Currents in the oceans are mainly driven by the density variation of seawater that is in turn determined by the salinity and temperature. Ocean salinity is therefore one of the key variables for monitoring and modeling ocean circulation. Ocean circulation and global water cycle are two most important components of the marine climate system. The interaction between the ocean circulation and the global water cycle affects the capacity of the oceans to store and release energy through precipitation, evaporation, and ocean circulation; it has thus an important regulating effect on global climate, resulting in changes to the ocean salinity (Lagerloef et al., 2008). SSS varies in response to evaporation, precipitation, snow/ice melt, river run-off on seasonal and/or interannual time scales. Since a change in the freshwater budget of oceanic mixed layer is reflected in the

SSS variability, SSS can be used to estimate surface freshwater flux. The relatively low salinity in the Indian Ocean is expected to affect the thermohaline circulation and ocean heat transport along the longitude in the mid-latitude sea areas (Yin et al., 2006a). The variations of the Indian Ocean's monsoon and dipole lead to changes in salinity (Sharma et al., 2010; Glejin et al., 2013), and the phenomenon can be better understood through observation of the salinity on a large scale. Studies on the variation of sea water salinity can make deeper understanding of ocean circulation, the global water cycle, and oceanic heat transport. However, there are limited salinity data in the high-latitude part of the Indian Ocean.

Remote observations of SSS have an important impact on the analysis of upper marine dynamics processes and air-sea interactions, since they provide a parametric basis for further understanding of the water and energy exchange in the oceans (Zhao et al., 2008). In addition, remote observations can provide data of SST and SSS on a regional to global scale, which can be used in

evaluations of sea surface circulation and oceanic numerical simulations.

Numerous studies have shown that L-band radiometry can be used for SSS retrieval (Yueh et al., 2001; Font et al., 2003; Camps et al., 2004; Yin et al., 2005; Lu et al., 2006; Shi et al., 2006; Lagerloef et al., 2008; Zhao et al., 2008; Wang et al., 2013). Based on these studies, satellites have been launched for observation of SSS from the space. The Soil Moisture and Ocean Salinity (SMOS) satellite was launched on November 2, 2009 by the European Space Agency (ESA) (Kerr et al., 2010), and the Aquarius/SAC-D (Satelite de Aplicaciones Cientificas-D) satellite was launched on June 10, 2011, in cooperation with the US National Aeronautics and Space Administration (NASA) and National Space Activities Commission (CONAE; Argentina) (Le Vine, 2011). These satellites greatly promote global observation of SSS by remote sensing technique.

SMOS carries its single payload, an L-band dual-polarization Microwave Imaging Radiometer by Aperture Synthesis (MIRAS), which has a frequency range of 1.400–1.427 GHz and is used to carry out multi-angle observations (Kerr et al., 2001). For the SMOS SSS products, Sabia et al. (2010) performed an ocean salinity error budget analysis on the SSS retrieved from SMOS and analyzed the effects of instrumental, external noise, geophysical parameters errors, multisource auxiliary SST, and wind speed data on SSS retrieval. Banks et al. (2012) reported a validation study in the Atlantic based on the SMOS monthly Level 3 products on a 1°×1° grid and found that the mean difference between the SMOS SSS and system Forecasting Ocean Assimilation Model-Nucleus for European Modelling of the Ocean (FOAM-NEMO) is around 0.90 practical salinity unit, decreasing to 0.50 in the North Atlantic subtropical zone. Wang et al. (2013) showed that the SSS retrieved from SMOS was slightly higher than the measured data, and the root mean square difference (RMSD) in the South China Sea and the Yellow Sea were 1.20 and 0.70, respectively. Based on the quality control data of the SSS retrieved from SMOS, Chen et al. (2014) analyzed the global error distribution of the salinity retrieved from SMOS and found that the errors of the retrieved SSS were relatively small in the tropical oceans but high in the high-latitude sea areas in the southern and northern hemispheres; they also indicated that the errors of SSS in the southern hemisphere were caused by the high wind speed and low temperature, and the errors of SSS at the continental margins were mainly caused by radio frequency interference (RFI). These asessment and evaluation activities, however, are mainly from SMOS SSS products.

For Aquarius SSS products, Reagan et al. (2014) analyzed the global and regional differences between SSS data obtained from the US National Oceanographic Data Center (NODC) and Aquarius SSS and revealed their similarities and differences within an annual cycle using the Fourier decomposition method. Reagan et al. (2013) performed a comparison study of the global distribution of SSS obtained from Aquarius against the *in situ* World Ocean Database (WOD) and found that the overall standard deviations in the areas from 0° to 15°, 15° to 30°, 30° to 45° and 45° to 60° in the southern hemisphere were 0.21, 0.14, 0.13 and 0.36, respectively. They also found that Aquarius products overestimated SSS in the high-salinity areas, and underestimated SSS in the low-salinity sea areas when compared with WOD-derived SSS. Ratheesh et al. (2014) verified the quality of SSS retrieved from Aquarius in the Indian Ocean (30°S–30°N, 35°–100°E) using the *in situ* data from Argo floats; correlation coefficient and RMSD were 0.84 and 0.45, respectively, and the spatial distribution and vari-

ation of Aquarius SSS were fairly consistent with the observations. Ebuchi and Abe (2012) conducted a global error analysis of the Aquarius SSS using the observation by Argo floats in the global oceans and showed that the Aquarius SSS was fairly consistent with the Argo data in the tropical zones and mid-latitude sea areas (RMSD was 0.60), whereas the RMSD was relatively large in high-latitude and low-temperature sea areas, with the values reaching 2.00. The objective of this study is to assess and adjust the Aquarius SSS data based on the *in situ* SSS measurements and MyOcean modeled SSS data.

2 Data and methods

2.1 *Study area*

The study area with the background of monthly mean SSS within the Indian Ocean in November 2012 is shown in Fig. 1. The positions of the *in situ* SSS measurement from the cruise are shown as white pentagram (2012) and black triangles (2013) within the black box. The mean salinity of the Indian Ocean is 34.76, and the SSS of the southeast Indian Ocean decreases with increasing latitude. The SSS values in the areas near 30°S, 40°S and 50°S are approximately 36.00, 35.00, and 34.00, respectively. The salinity mainly depends on evaporation and precipitation in the ocean, their differences in the areas near 30°S, 40°S and 50°S are 100.0, 25.0, and –50.0 g/cm², respectively (Feng et al., 1999).

The sea surface temperature (SST) distribution of the Indian Ocean varies with latitude. SSTs in the austral summer in the areas near 20°S, 30°S, 40°S and 50°S in the southeast are 25–27°C, 20–22°C, approximately 15°C and approximately 0°C, respectively; SSTs in the austral winter in the areas near 20°S, 30°S, 40°S
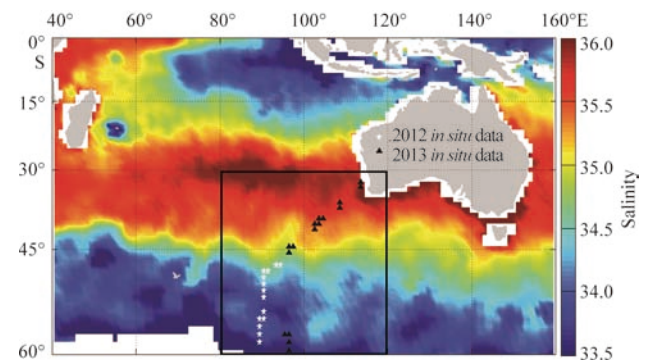
Fig. 1. The study area with the background of monthly mean sea surface salinity (SSS) (November 2012). The positions of the *in situ* SSS measurement from the cruise are shown as white pentagram (November 2012) and black triangles (March 2013) within the black box.

and 50°S in the southeast are 22–23°C, 15–17°C, 12–13°C and approximately 0°C, respectively (Xie et al., 2002). The sensitivity of brightness temperature (T_B) to SSS is significantly related to SST, and the sensitivities at 20°C and 0°C are 0.50°C/psu and 0.25°C/psu, respectively (Lerner and Hollinger, 1977; Kerr et al., 2010). The decrease in sensitivity can result in a larger error in the retrieval of SSS in low-temperature areas (Yueh et al., 2001; Boutin et al., 2012).

The annual wind field over the south Indian Ocean is relatively stable. The wind speed varies with latitude. The annual mean wind speed in the western wind belt is higher than 8.0 m/s,

and the wind speed in the area between 40°S and 50°S is the highest with an average of 10.0–12.0 m/s (Liang et al., 2003). A water-body-convergence zone exists in the area with a relatively high wind speed in the southeast Indian Ocean (Luis and Pandey, 2005). The actual microwave radiation from the ocean surface consists of radiation from the flat sea surface and sea waves. The sensitivity of T_B to wind speed at nadir is approximately 0.23–0.25 °C/(m·s⁻¹); an increase in T_B caused by high wind speed results in a relatively lower value of the retrieved SSS and the larger error (Camps et al., 2004).

2.2 *In situ SSS*

During the 29th Chinese Antarctic Expedition (from November 2012 to March 2013), temperature and salinity data of the sea surface were collected by CTD in the southeast Indian Ocean, concurrently with the Aquarius data acquisition. The daily data are averaged (mean value) into a 1°×1° grid between longitudes 80°–120°E and latitudes 30°–60°S. Then, the concurrent SSS from

the Aquarius/SAC-D satellite and the *in situ* SSS are co-located and paired on a daily basis. The positions of the conductivity, temperature, and depth (CTD) stations where SST and SSS data have been co-located are shown in Fig. 1. The position of each mean of *in situ* SSS value shown in Fig. 1 is also the center of each pixel. Consequently, there are 14 pixels matched in November 2012, 16 pixels in March 2013. The *in situ* data are showed in Fig. 2, along with the co-located Aquarius SSS data.

2.3 *Aquarius data*

The Aquarius/SAC-D satellite is primarily designed to monitor the global SSS, and it circulates in a sun-synchronous orbit 657 km above the earth's surface. Global coverage is completed every seven days in 103 orbits, and it measures SSS using a passive/active L- and S-band (PALS) sensor, which is a combination of L-band radiometer (1.413 GHz) and scatterometer (1.26 GHz) (Lagerloef et al., 2008; Lagerloef, 2012). The main scientific objective of Aquarius is to record seasonal and annual variations of SSS in
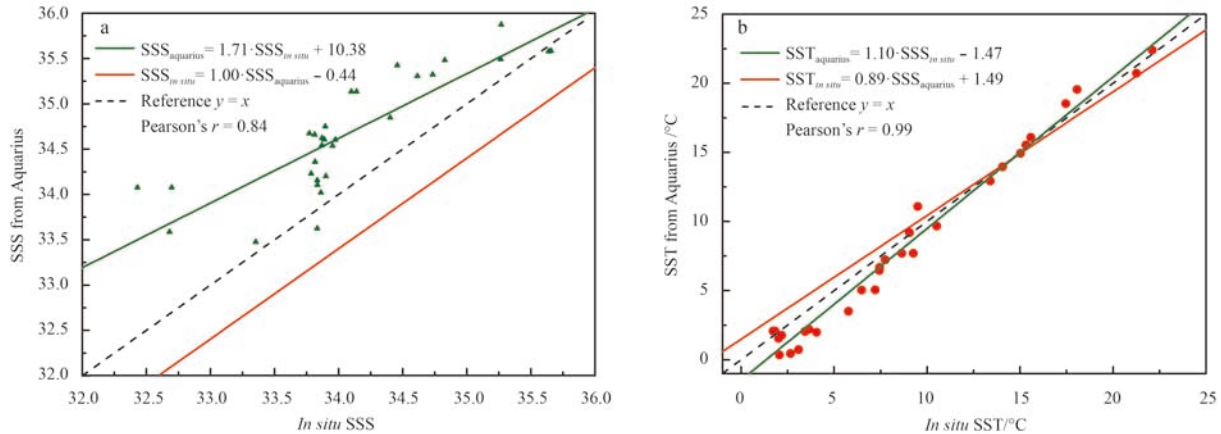
Fig. 2. Aquarius versus the *in situ* sea surface salinity (SSS) (a); and Aquarius versus the *in situ* sea surface temperature (SST) (b).

the open sea around the globe and provide data on the temporal resolution (30 days), spatial resolution (150 km) and global mean SSS with a mean accuracy of 0.20 when random errors and deviations are considered (Le Vine et al., 2007; 2010).

Salinity changes the emissivity of seawater in the microwave spectral region because it influences dielectric constant (Le Vine, 2011), and the L-band sensor on Aquarius monitors such changes. After eliminating interference caused by galactic radiation, the Faraday rotation of the ionosphere, atmospheric attenuation, and RFI, the sea surface brightness temperature can be obtained from the microwave radiation detected by the antennas. The SSS is then calculated using the following equation (Wentz and Le Vine, 2008).

$$S = s_0\left(\theta_i, t_s\right) + s_1\left(\theta_i, t_s\right) T_{\text{BV,sur}} + s_2\left(\theta_i, t_s\right) T_{\text{BH,sur}} + s_3\left(\theta_i, t_s\right) W, \tag{1}$$

where S represents SSS; θ_i for incident angle (range 25.0°–50.0°; step size 0.1°); t_s for SST (°C) (range –5.0–40.0°C; step size 0.1°C); $T_{\text{BH,sur}}$ represents the sea surface brightness temperature (K) of vertical polarization; $T_{\text{BH,sur}}$ for the brightness temperature (K) of horizontal polarization; and W for sea surface wind speed (m/s) (Meissner et al., 2012). The s coefficients (included s_0, s_1, s_2) are functions of θ_i and t_s and are in tabular form. The algorithm is trained by deriving a set of s coefficients that minimize the vari-

ance between the salinity S given by Eq. (1) and the true salinity (Meissner et al., 2012).

Level-3 standard mapped image (SMI) products are used, including the orbital data of daily salinity, SST, and wind fields in the southeast Indian Ocean from November 2012 to March 2013, and the monthly mean SSS and wind field data of the southeast Indian Ocean in November 2012 (spatial grid of 1°×1°). The aforementioned data are processed by the software of SimGEN 4.3. The daily data is V2.9, and the monthly wind and SSS data are V3 and V2, respectively. The SST products with spatial resolution of 1°×1° in November 2012 are originated from National Oceanic and Atmospheric Administration (NOAA), which are processed by NOAA using the interpolation method based on the station and satellite remote sensing data (Reynolds et al., 2002).

2.4 *MyOcean data*

MyOcean is the first implemented project of the integrated pan-European Marine Core Service for ocean monitoring and forecasting. It provides access to a lot of observation-based and model-based products (Bahurel et al., 2010). MyOcean reanalysis data for the global oceans are generated by assimilating all different types of available data sets: the Argo profiling floats, the moored buoys, remote sensing measurements, and simulation datasets (Nardelli et al., 2013). The MyOcean reanalysis data include real-time and delayed SST and SSS data, which can effect-

ively improve the capacity of ocean monitoring and forecasting (Guinehut et al., 2012). Many studies proved that the model data are in good agreement with the observed data, and they can be used as ground truth for satellite data (Cheng et al., 2012; Guinehut et al., 2012; Nardelli et al., 2013).

MyOcean data with spatial resolution of (1/3)°×(1/3)° is the modeled products of the version 1 ARMOD-3D (SSS of November 2012). The weekly data sets are averaged into monthly data and the average of nine pixels is as the new one to resample onto a coarser grid. Then, the MyOcean data, concurrent with the *in situ* and Aquarius SSS data sets, are used to evaluate the Aquarius SSS in November 2012 before and after adjustment.

2.5 *Data processing*

Data processing mainly consists of six steps. (1) *In situ* and satellite data format conversion. The *in situ* SSS in the hexadecimal (HEX) format measured using a CTD are converted to the ASCII format (copy number variant, CNV), and the Aquarius image data are converted to Network Common Data Form (NetCDF, NC) format. (2) Extract the ROI from the data. The data between longitudes 80°–120°E and latitudes 30°–60°S are extracted from the raw data. (3) Data matching. For each day, the position of each *in situ* SSS data point from the cruise must be located in the daily Aquarius image of the same day. If the multiple *in situ* SSS data points lie within the same pixel, then the average is taken as the *in situ* SSS corresponding to the pixel. (4) Formulate adjustment scheme. The co-located data sets (Aquarius SSS versus the *in situ* SSS) are analyzed by regression, and the correction equation is as follows with R^2=0.73, *RMSE*=0.40.

$$S_{\text{adjusted}} = 0.35 S_{\text{aqua}}^2 - 23.25 S_{\text{aqua}} + 419.70, \qquad (2)$$

where S_{adjusted} represents the adjusted Aquarius SSS, and S_{aqua} is the raw Aquarius SSS. (5) Adjusting the Aquarius SSS products. The Aquarius SSS products (November, 2012) are adjusted based on the adjustment scheme. Then, the MyOcean data are used to assess the adjusted SSS. (6) Assessing the adjusted SSS with MyOcean. The differences between the Aquarius SSS before and after adjustment and the spatial distribution characteristics of the difference are analyzed.

3 Results and discussion

### 3.1 *Comparison of Aquarius SSS with the in situ SSS*

The Aquarius SSS values are mainly in the range of

33.50–36.00, whereas the *in situ* SSS are in the range of 33.00–35.50. Regression analysis is performed between Aquarius and the *in situ* measurement for SSS and SST, and the results are shown in Fig. 2. There is a strong positive correlation between the Aquarius SSS and the *in situ* SSS with correlation coefficient r=0.84 and significance level p-value<0.01 (Fig. 2 a). The correlation between the Aquarius SST and the *in situ* SST is even higher with r=0.99 and p-value<0.01 (Fig. 2b). These results may show that the Aquarius SSS and SST in the area are overall consistent with the *in situ* measurements. Compared with the *in situ* SSS, the RMSD of the Aquarius SSS in the southeast Indian Ocean is approximately 0.44 (Fig. 2a), which is generally consistent with the previous research results (Lagerloef et al., 2008; Ebuchi and Abe, 2012).

The difference (Aquarius minus the *in situ* measurement) versus the Aquarius SSS is shown in Fig. 3 a. By calculating the RMSD of the difference for Aquarius SSS less than 34.20, and greater than 34.20, the RMSD of them are 0.84 and 0.67, respectively. It shows that the difference is higher in relatively low salinity area. The difference versus the wind velocity from the scatterometer onboard Aquarius is shown in Fig. 3 b. When the wind speed is larger than 12 m/s, the difference is higher. Wentz and Le Vine (2008) separated the impact of wind speed on the Aquarius SSS into two components: a random component and a linear component in which the difference increases linearly with the Aquarius SSS; the random component might be related to the random pattern of wind direction. Although the wind velocity retrieved from the scatterometer on Aquarius is used to obtain the SSS, the correlation analysis between the wind speed and Aquarius SSS indicates that the effect is not completely eliminated (Fig. 3b). Wind speed increases the T_B of the L-band radiometer by influencing the sea surface roughness and thus the scattering of the microwave. Increases in brightness temperature are usually linearly related to the wind speed, and a regression analysis can partially eliminate the effect of wind speed to increase the accuracy of the Aquarius SSS (Yin et al., 2006b).

3.2 *Comparison of Aquarius SSS before and after adjustment*

The adjustment equation is applied to the monthly L3 SMI Aquarius data in November 2012 and the SSS difference between the adjusted and non-adjusted data in November 2012 are being displayed in Fig. 4. The adjusted Aquarius SSS is obtained by adding the adjustment value to the Aquarius SSS for each pixel.
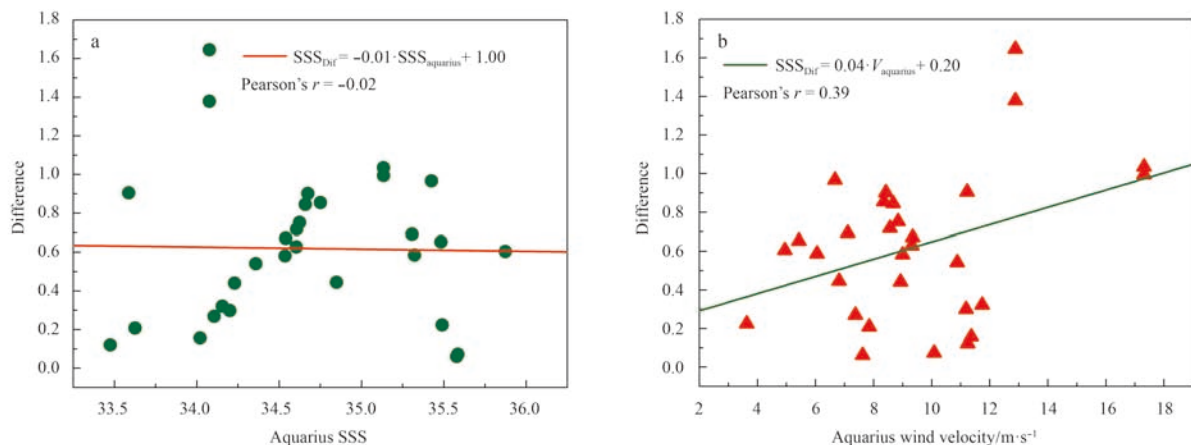
Fig. 3. The difference of sea surface salinity (SSS) is defined as the Aquarius SSS minus the *in situ* SSS: a. difference versus the Aquarius SSS and b. difference versus the Aquarius scatterometer's wind velocity.
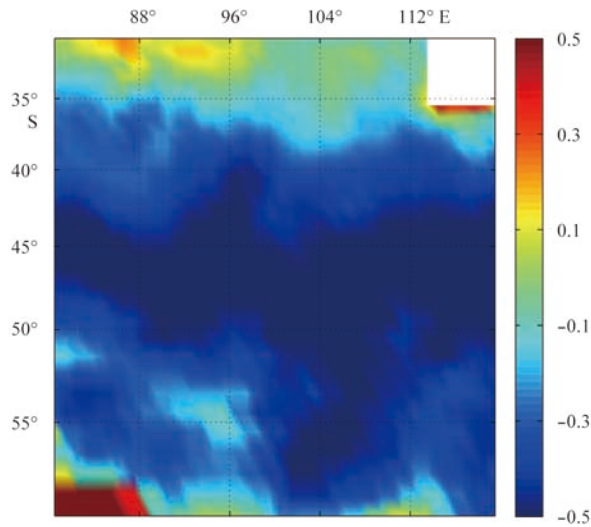
Fig. 4. The spatial distribution of the adjustment (adjusted Aquarius sea surface salinity (SSS) minus the Aquarius SSS).

In the southeast Indian Ocean between 35° and 55°S, the value is mostly negative. It means that the adjusted Aquarius SSS is smaller than the unadjusted in this area. Most positive adjustment values occur in area north of 35°S and south of 55°S.

The mean value of adjustment is –0.26 and the range is between –0.55 and+0.55. Near the latitude 45°S, the adjustment or the difference between the Aquarius SSS after and before adjustment is approximately –0.5. Since the most sampling points are near the 45°S, the adjusted Aquarius SSS are closer to the *in situ* and MyOcean modeled SSS in area around 45°S (Figs 5b and c).

3.3 *Comparison of Aquarius SSS with MyOcean SSS*

3.3.1 *Distribution of zonal mean*

The relationship between SSS of different origins (cases) and latitude in the southeast Indian Ocean is shown in Fig. 6. This comparison between the monthly MyOcean data and the monthly adjusted/non-adjusted Aquarius SSS is for November 2012. It is apparent that the salinity decreases with increasing latitude for all cases, which is consistent with the normal latitudinal distribution pattern of SSS (Feng et al., 1999). In the southeast Indian Ocean between 30°S and 45°S, the Aquarius SSS is generally higher than the MyOcean modeled SSS by approximately 0.40. In the southeast Indian Ocean between 46°S and 50°S, the Aquarius SSS is closer to the MyOcean SSS, and the difference is between 0.10 and 0.20. In the southeast Indian Ocean above about 53°S, the Aquarius SSS and the MyOcean SSS are almost the same. The MyOcean SSS is close to the Aquarius SSS in the relatively high-latitude sea area, and the adjusted Aquarius SSS generally matches the MyOcean SSS in the ocean between 38°S and 45°S (Fig. 6). The adjustment works well in the range of 34.00 to 35.50, with the difference being mostly less than 0.20. The difference
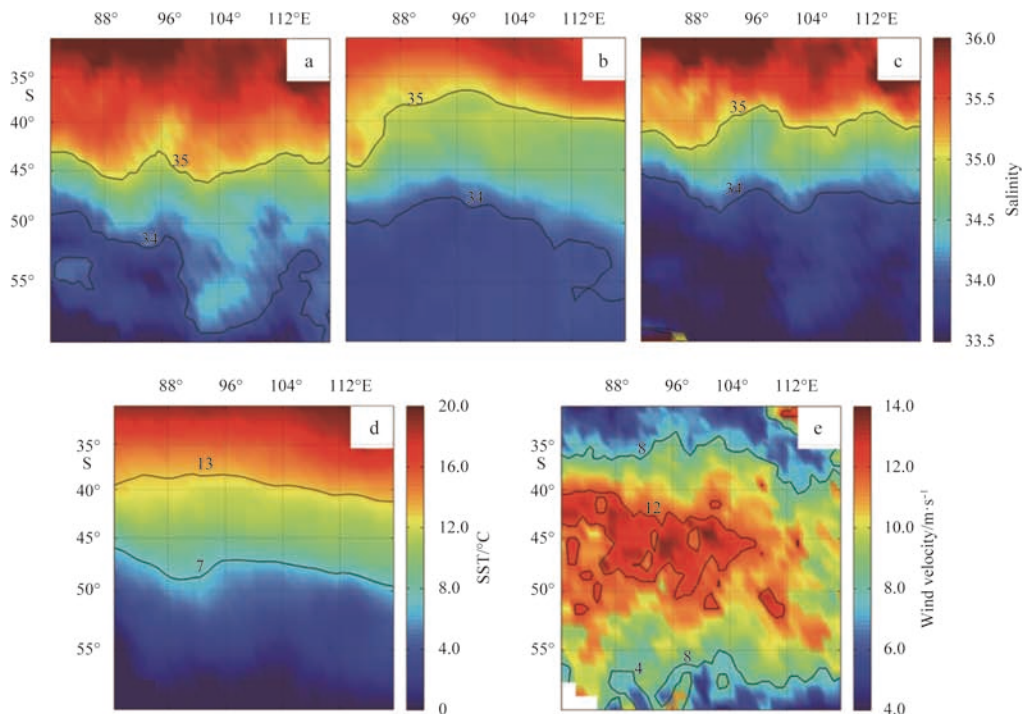
Fig. 5. The spatial distribution of sea surface salinity (SSS) in the southeast Indian Ocean in November 2012. a. SSS from the Aquarius, b. SSS from the MyOcean data, c. adjusted SSS from the Aquarius using the measured data as reference, d. sea surface temperature (SST) from NOAA_OI_SST_V2 data provided by the NOAA; and e. wind velocity from the Aquarius scatterometer.

between the adjusted Aquarius SSS and the MyOcean SSS is over 0.20 in the southeast Indian Ocean north of 35°S, and the difference is the smallest in the area near 41°S. The adjusted Aquarius SSS is lower than the MyOcean SSS by more than 0.30 in the area south of 47°S. The variation characteristics of the adjusted Aquarius SSS seem to be related to the distribution of the *in situ*
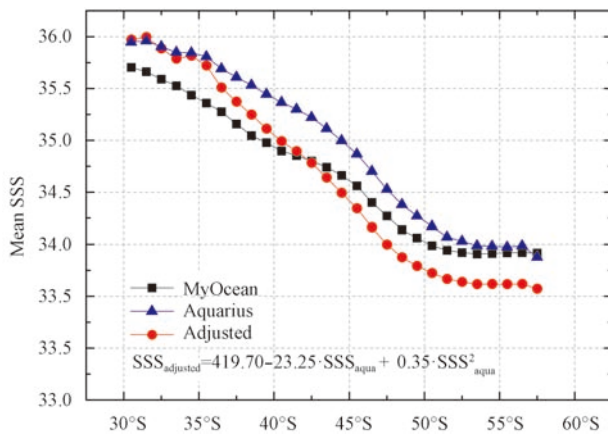
Fig. 6. The sea surface salinity (SSS) variation with latitude in the southeast Indian Ocean.

from the two cruise segments. It could benefit this study to utilize more hydrographic data from this region (i.e., Argo floats).

3.3.2 *Spatial distribution of disparity*

For convenience in the following discussion, "the Aquarius SSS" refers to the Aquarius SSS before adjustment, and "the adjusted Aquarius SSS" refers to the Aquarius SSS after adjustment. Overall, most of the disparity between the Aquarius SSS and the MyOcean SSS in the southeast Indian Ocean between 35°S and 50°S are greater than 0.40 (Fig. 7a), and the corresponding wind speeds are mostly higher than 8.0 m/s, with wind speed in high-wind areas greater than 12.0 m/s (Fig. 5e). The difference between the adjusted SSS and the MyOcean SSS in high-wind areas is less than 0.40 in most sea areas (Fig. 7b). The water in the southeast Indian Ocean south of 55°S and west of 98°E is cold (approximately 0.0°C) (Fig. 5d), and the Aquarius SSS is lower than the MyOcean SSS (Figs 5a and b). The mean wind speed is relatively low in the southeast Indian Ocean south of 55°S and
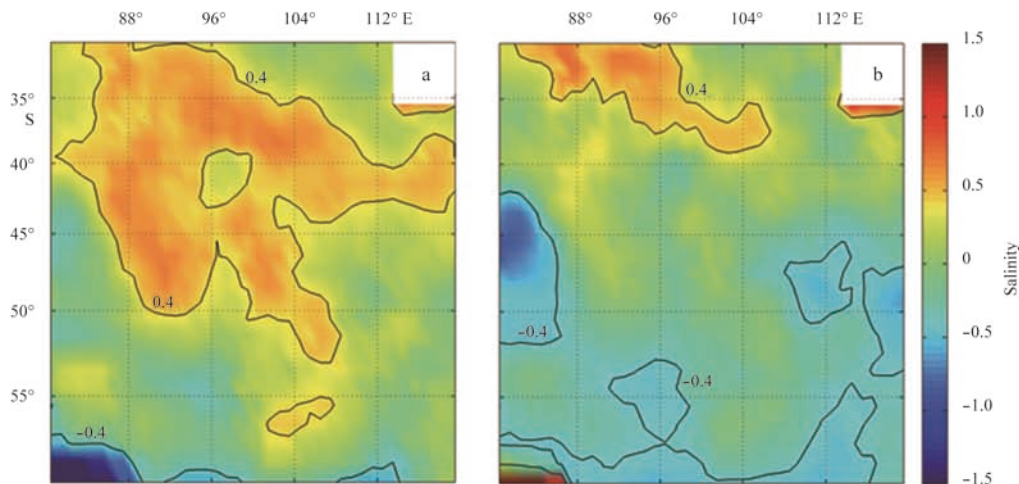
Fig. 7. The spatial distribution of disparity. The difference between Aquarius and the MyOcean sea surface salinity (SSS) (a) and the difference between the adjusted Aquarius SSS and the MyOcean SSS (b).

sampling locations and the difference is large in areas with fewer samplings.

In the southeast Indian Ocean, the mean SSS value of those retrieved from Aquarius, obtained from the MyOcean model, and of the adjusted salinity of the whole study area is 34.83, 34.61, and 34.57, respectively. The mean value of the adjusted Aquarius SSS is closer to the MyOcean SSS than the unadjusted Aquarius SSS. Compared with the MyOcean modeled data, adjustment reduces the mean absolute differences of Aquarius SSS from 0.31 before adjustment to 0.25 after adjustment.

In general, the Aquarius SSS is found to be higher than the MyOcean SSS in the mid- to low-latitude of the southeast Indian Ocean, and the average difference is about 0.42; relatively high wind speed within each pixel in the mid- to low- latitude southeast Indian Ocean maybe contribute to such difference. The adjusted SSS is fairly consistent with the characteristics of the SSS data from the MyOcean model. For instance, the difference between the adjusted Aquarius SSS and the MyOcean SSS is very small or even zero in the area at or near 41°S because of the higher number of samplings in this sea area (Fig. 6). The difference is within 0.50 in other sea areas. This study is based on limited (30) co-located data points between Aquarius and the *in situ* data

east of 98°E.

There is a sea area of high-salinity in the south of 36°S and east of 112°E (Figs 5a and c), and the mean absolute error (MAE) of the Aquarius SSS is approximately 1.00 when compared with MyOcean SSS (Figs 7a and b), which is consistent with previous research results (Yueh et al., 2001; Wang et al., 2013). The potential cause of the error is perhaps the land contamination in this region.

A comparison between the Aquarius SSS and the MyOcean data in the southeast Indian Ocean north of 35°S shows that Aquarius SSS value is consistently higher in the sea area west of 100°E with an average difference of about 0.40 (Fig. 7a), whereas the difference is relatively small in the sea area east of 100°E (Fig. 7a). There is no change in the overall distribution pattern of the SSS after adjustment (Figs 5a, b and c). The *in situ* SSS based on a November climatology in the sea area near 40°S is 35.00 (Feng et al., 1999) and consistent with the 35.00 contour of MyOcean SSS (Fig. 5b), which indicates that the MyOcean data matches well with the *in situ* measurement. However, the 35.00 contour of the Aquarius SSS shifts southward (Fig. 5a). Since SSS values decrease southward, the shift indicates that the Aquarius SSS in the sea area is overestimated in general and the SSS difference is

greater than 0.40 (Fig. 7a), when compared with the MyOcean SSS. The adjusted Aquarius SSS matches generally well with the MyOcean SSS (Figs 5b and c) with difference lower than 0.40 (Fig. 7b). The adjusted Aquarius SSS matches well with the MyOcean SSS in the southeast Indian Ocean near 50°S and west of 98°E, although there is a low-salinity water jet in the sea area near 50°S and 96°E (Figs 7a and b). It appears there is also a low-salinity water jet at 82°E and 45°S. Both of these features are worsened through the adjustment scheme when compared to the non-adjusted Aquarius SSS. The reasons may be the lower SST and an unstable adjustment scheme apart from these feature, the overall characteristics of the adjusted SSS are similar to the MyOcean model simulation results (Figs 5b and c).

The variation amplitude of the Aquarius SSS, MyOcean SSS, and adjusted Aquarius SSS for the entire sea area of the southeast Indian Ocean is approximately 8.81, 2.03, and 7.01, respectively. The difference between the Aquarius SSS and the MyOcean modeled SSS is mostly distributed between 0.00 and 0.50, and the mean of the difference is 0.21 and the variance is 0.49. Compared with the MyOcean modeled SSS, the mean of the difference after adjustment becomes –0.05 and the variance is 0.49. It is interesting to note that while the bias is greatly improved through the adjustment scheme, the variance remains the same. The reasons may be that in retrieval of SSS from remote sensing sensors, system noise and environmental background noise can produce random errors of Gaussian distributions, and the adjustment scheme only makes the mean of difference to negative direction. The differences between the Aquarius SSS and MyOcean SSS are all greater than 0.40 in the high-wind-speed sea areas (40°–52°S, 88°–106°E), whereas the difference becomes significantly lower

than 0.40 after adjustment, indicating that the difference in high-wind-speed sea areas could be reduced through adjusting the Aquarius SSS using the adjustment scheme. The performance of the adjustment becomes poorer in the sea areas where there are few samplings. It is expected that the denser of the *in situ* SSS measurements overlapping with the Aquarius in a specific area, the more typical the adjustment scheme and the better the adjusted Aquarius SSS would be.

Most of the differences between the Aquarius SSS and MyOcean SSS in the southeast Indian Ocean are between –0.50 and 0.50; the mean difference from 0–8 m/s and >8 m/s are 0.19 and 0.25 (Fig. 8a). The difference between the adjusted SSS and MyOcean SSS are distributed almost symmetrically about zero-difference axis (Fig. 8c); and the mean difference from 0–8 m/s and>8 m/s are 0.08 and –0.12. Under different wind speed conditions, the change of the mean difference can be seen that the adjustment scheme can suppress the influence of wind speed. The difference versus SST is shown in Fig. 8b. With respect to the MyOcean SSS, the mean difference from <6°C for the non-adjusted and adjusted Aquarius SSS are 0.23 and 0.11. This also shows that the adjustment scheme may be useful for the low-temperature sea areas. In low-temperature (0.0°C) sea areas, the variation amplitude of the SSS difference is approximately 2.00 (Fig. 8b), which is consistent with previous research results (Ebuchi and Abe, 2012). The variation amplitude of the SSS difference in low-temperature sea areas decreases to some extent after adjustment (Fig. 8d). The SST is 6.0–12.0°C in the sea area between 40°S and 50°S (Fig. 5d), and the perennial wind speed becomes relatively high (Fig. 5e); therefore, the difference between 0.00 and 0.50 is relatively dispersed (Fig. 8b).
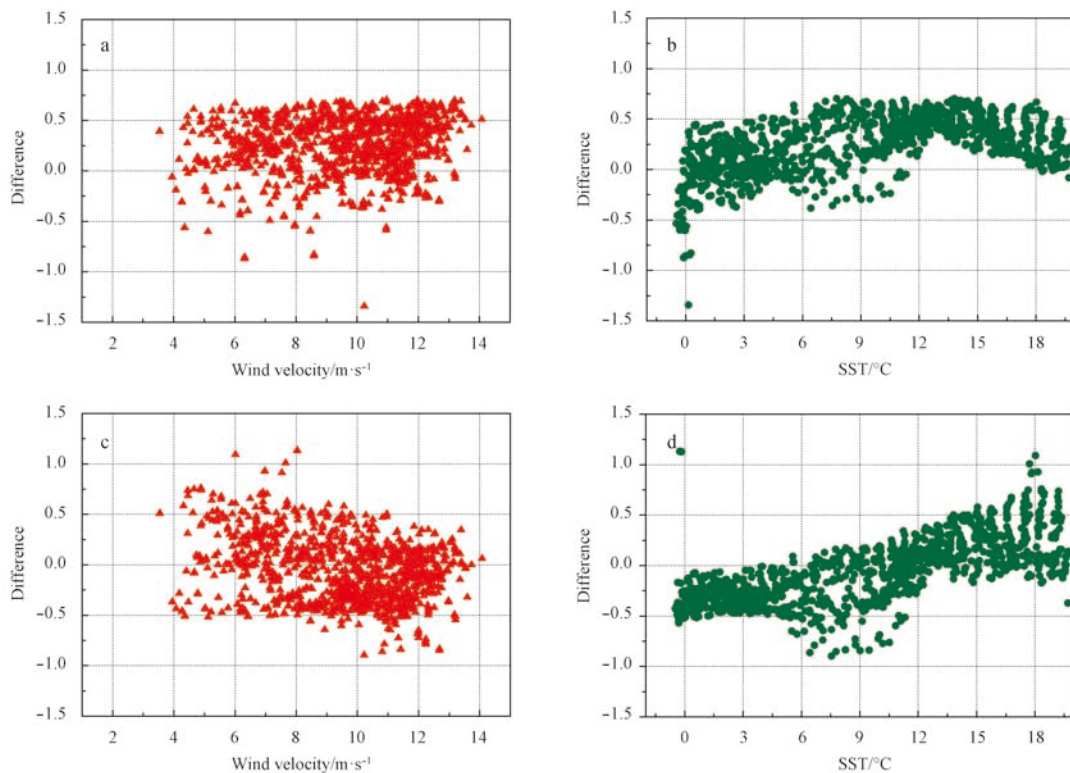
Fig. 8. Relationship between the difference (Aquarius sea surface salinity (SSS) minus MyOcean SSS) and wind velocity and sea surface temperature (SST). Difference versus wind velocity before adjustment (a), difference versus SST before adjustment (b), difference versus wind velocity after adjustment (c), and difference versus SST after adjustment (d).

4 Conclusions

Based on the significant correlation between the Aquarius SSS and the *in situ* measurement of SSS from a cruise to the Indian Ocean, and corrections of wind and SST effects on SSS, the Aquarius SSS has been adjusted and assessed using MyOcean modeled SSS. Overall, the monthly mean products of the Aquarius SSS show that SSS values in the southeast Indian Ocean are high, but they are low in some local sea areas. The mean value of the difference between the Aquarius SSS and the MyOcean modeled SSS is 0.42. In the sea area between 40° and 50°S, there is a perennially high wind in the western zone with mean wind speed of 12.0 m/s. The difference can be up to 1.00 and the mean value of 0.40. Since retrieval of SSS from microwave brightness temperature is sensitive to the value of SST, the cold water in the sea area south of 55°S and west of 98°E reduces the sensitivity of SSS to SST; therefore, the SSS difference in this sea area can be up to 2.00 while the Aquarius SSS values are on the contrary low.

Compared with the MyOcean SSS, the adjustment of the Aquarius SSS using the *in situ* measured SSS from a scientific cruise in the sea area (40°–52°S, 88°–106°E) is conducive to reduce the difference. With increasing wind speed, the difference exhibits a normal distribution after adjustment. The adjustment scheme effectively improves the accuracy of the retrieved SSS in the corresponding sea area and reduces the large error caused by high wind speed. However, in the sea area north of 35°S and south of 55°S, the adjustment scheme is not particularly effective mainly possibly due to limited number of SSS samplings in that area.

In summary, we assess the Aquarius SSS L3 products in the southeast Indian Ocean based on the *in situ* SSS measurement from a scientific cruise. An adjustment scheme has been developed to adjust the Aquarius SSS taken the *in situ* measurement as the reference. The adjusted Aquarius SSS is compared with the MyOcean data. Results show that: (1) the mean difference between the Aquarius SSS and the *in situ* SSS is 0.42; (2) the magnitude of the mean difference between the Aquarius SSS and MyOcean SSS is reduced from 0.21 to –0.05 after adjustment; (3) the variation amplitude of the difference after adjustment becomes smaller, and the absolute difference of the SSS is within 0.40; (4) although the data points from the cruise are limited, the results are encouraging given the challenges associated with improving the accuracy of observing the SSS from remotely sensed data.

References

Bahurel P, Adragna F, Bell M J, et al. 2010. Ocean Monitoring and Forecasting Core Services: The European MyOcean Example. In: Hall J, Harrison D E, Stammer, D, Eds. Proceedings of OCEANOBS'09 Sustained Ocean Observations and Information for Society. Venice, Italy: ESA Publication WPP-306, 2–11

Banks C J, Gommenginger C P, Srokosz M A, et al. 2012. Validating SMOS ocean surface salinity in the Atlantic with Argo and operational ocean model data. IEEE Transactions on Geoscience and Remote Sensing, 50(5): 1688–1702

Boutin J, Martin N, Yin Xiaobin, et al. 2012. First assessment of SMOS data over open ocean: Part II Sea surface salinity. IEEE Transactions on Geoscience and Remote Sensing, 50(5): 1662–1675

Camps A, Font J, Vall-llossera M, et al. 2004. The WISE 2000 and 2001 field experiments in support of the SMOS Mission: Sea surface L-Band brightness temperature observations and their application to sea surface salinity retrieval. IEEE Transactions on Geoscience and Remote Sensing, 42(4): 804–823

Chen Jian, Zhang Ren, Wang Huizan, et al. 2014. An analysis on the error structure and mechanism of soil moisture and ocean salinity remotely sensed sea surface salinity products. Acta Oceanologica Sinica, 33(1): 48–55

Cheng Y, Andersen O B, Knudsen P. 2012. First evaluation of MyOcean altimetric data in the Arctic Ocean. Ocean Science Discussions, 9(1): 291–314

Ebuchi N, Abe H. 2012. Evaluation of sea surface salinity observed by Aquarius. In: 2012IEEE International Geoscience and Remote Sensing Symposium (IGARSS). Munich: IEEE, 5767–5769

Feng Shizuo, Li Fengqi, Li Shaoqing. 1999. An Introduction to Marine Science (in Chinese). Beijing: The Higher Education Press, 83–108

Font J, Lagerloef G, Le Vine D, et al. 2003. The determination of surface salinity with SMOS-recent results and main issues. In: Proceedings of 2003 IEEE International Geoscience and Remote Sensing Symposium (IGARSS'03). Toulouse, France: IEEE, 7–9

Glejin J, Kumar V S, Nair T M B. 2013. Monsoon and cyclone induced wave climate over the near shore waters off Puduchery, south western Bay of Bengal. Ocean Engineering, 72: 277–286

Guinehut S, Dhomps A L, Larnicol G, et al. 2012. High resolution 3-D temperature and salinity fields derived from in situ and satellite observations. Ocean Science, 8(5): 845–857

Kerr Y H, Waldteufel P, Wigneron J P, et al. 2001. Soil moisture retrieval from space: The Soil Moisture and Ocean Salinity (SMOS) mission. IEEE Transactions on Geoscience and Remote Sensing, 39(8): 1729–1735

Kerr Y H, Waldteufel P, Wigneron J P, et al. 2010. The SMOS Mission: New tool for monitoring key elements of the global water cycle. Proceedings of the IEEE, 98(5): 666–68

Lagerloef G. 2012. Satellite mission monitors ocean surface salinity. Eos, Transacations American Geophysical Union, 93(25): 233–234

Lagerloef G, Colomb F R, Le Vine D, et al. 2008. The Aquarius/SAC-D Mission: Designed to meet the salinity remote-sensing challenge. Oceanography, 21(1): 68–81

Lerner R M, Hollinger J P. 1977. Analysis of 1.4 GHz radiometric measurements from Skylab. Remote Sensing of Environment, 6(4): 251–269

Le Vine D M , Lagerloef G S E, Colomb F R, et al. 2007. Aquarius: An instrument to monitor sea surface salinity from space. IEEE Transactions on Geoscience and Remote Sensing, 45(7): 2040–2050

Le Vine D M, Lagerloef G S E, Torrusio S E. 2010. Aquarius and remote sensing of sea surface salinity from space. Proceedings of the IEEE, 98(5): 688–703

Le Vine D M. 2011. Aquarius Instrument and Salinity Retrieval. http://aquarius.umaine.edu/cgi/documents.htm [03-Jun-2011]

Liang Yuqing, Liu Jinfang, Zhang Xian, et al. 2003. Temporal and spatial characteristics of South Indian Ocean wind field. Marine Forecasts (in Chinese), 20(1): 25–31

Lu Zhaoshi, Shi Jiuxin, Jiao Yutian, et al. 2006. Experimental study of microwave remote sensing of sea surface salinity. Ocean Technology (in Chinese), 25(3): 70–75, 89

Luis A J, Pandey P C. 2005. Characteristics of atmospheric divergence and convergence in the Indian Ocean inferred from scatterometer winds. Remote Sensing of Environment, 97(2): 231–237

Meissner T, Wentz F, Lagerloef G, et al. 2012. The Aquarius salinity retrieval algorithm. In: 2012 12th Specialist Meeting on Microwave Radiometry and Remote Sensing of the Environment. Rome: IEEE, 1–3

Nardelli B B, Tronconi C, Pisano A, et al. 2013. High and Ultra-High resolution processing of satellite Sea Surface Temperature data

over Southern European Seas in the framework of MyOcean project. Remote Sensing of Environment, 129: 1–16

Ratheesh S, Sharma R, Sikhakolli R, et al. 2014. Assessing sea surface salinity derived by Aquarius in the Indian Ocean. IEEE Geoscience and Remote Sensing Letters, 11(4): 719–722

Reagan J, Boyer T, Antonov J. 2013. Comparison analysis between Aquarius sea surface salinity and world ocean database *in situ* analyzed sea surface salinity.http://aquarius.umeoce.maine.edu/docs/aqsci2013_reagan.pdf [2013–11]

Reagan J, Boyer T, Antonov J. 2014. Comparison analysis between Aquarius sea surface salinity and World Ocean Database in situ analyzed sea surface salinity. Journal of Geophysical Research: Oceans, 119(11): 8122–8140

Reynolds R W, Rayner N A, Smith T M, et al. 2002. An improved in situ and satellite SST analysis for climate. Journal of Climate, 15(13): 1609–1625

Sabia R, Camps A, Talone M, et al. 2010. Determination of the sea surface salinity error budget in the Soil Moisture and Ocean Salinity Mission. IEEE Transactions on Geoscience and Remote Sensing, 48(4): 1684–1693

mitt R W. 2008. Salinity and the global water cycle. Oceanography, 21(1): 12–19

Sharma R, Agarwal N, Momin I M, et al. 2010. Simulated sea surface salinity variability in the Tropical Indian Ocean. Journal of Climate, 23(24): 6542–6554

Shi Jiuxin, Lu Zhaoshi, Li Shujiang, et al. 2006. Retrieval algorithm for seawater's salinity and temperature by L and S band microwave remote sensing. Chinese High Technology Letters (in Chinese), 16(11): 1181–1184

Wang Xinxin, Yang Jianhong, Zhao Dongzhi, et al. 2013. SMOS satellite salinity data accuracy assessment in the China coastal areas. Haiyang Xuebao (in Chinese), 35(5): 169–176

Wentz F J, Le Vine D. 2008. Algorithm theoretical basis document Aquarius level-2 radiometer algorithm: Revision 1. RSS Technical Report 012208, http://oceancolor.gsfc.nasa.gov/AQUARIUS/DOCS/Level2_salinity_atbd_rev1.pdf

Xie Shangping, Annamalai H, Schott F A, et al. 2002. Structure and mechanisms of South Indian Ocean climate variability. Journal of Climate, 15(8): 864–878

Yin Xiaobin, Liu Yuguang, Zhang Hande, et al. 2005. Microwave remote sensing of sea surface salinity—A study on microwave radiation theory of calm sea surface. Chinese High Technology Letters (in Chinese), 15(8): 86–90

Yin Xiaobin, Liu Yuguang, Zhang Hande. 2006a. Removing the impact of wind direction on remote sensing of sea surface salinity. Chinese Science Bulletin, 51(11): 1368–1373

Yin Xiaobin, Liu Yuguang, Zhang Hande. 2006b. Removing the impact of wind direction on remote sensing of sea surface salinity. Chinese Science Bulletin (in Chinese), 51(3): 349–354

Yueh S H, West R, Wilson W J, et al. 2001. Error sources and feasibility for microwave remote sensing of ocean surface salinity. IEEE Transactions on Geoscience and Remote Sensing, 39(5): 1049–1060

Zhao Kai, Shi Jiuxin, Zhang Hande. 2008. High sensitivity airborne L-band microwave radiometer measurements of sea surface salinity. Journal of Remote Sensing (in Chinese), 12(2): 277–283